Point mutations alter the mechanical stability of immunoglobulin modules

Hongbin Li, Mariano Carrion-Vazquez, Andres F. Oberhauser, Piotr E. Marszalek and Julio M. Fernandez

Department of Physiology and Biophysics, Mayo Foundation, Rochester, Minnesota 55905, USA.

Immunoglobulin-like modules are common components of proteins that play mechanical roles in cells such as muscle elasticity and cell adhesion. Mutations in these proteins may affect their mechanical stability and thus may compromise their function. Using single molecule atomic force microscopy (AFM) and protein engineering, we demonstrate that point mutations in two β-strands of an immunoglobulin module in human cardiac titin alter the mechanical stability of the protein, resulting in mechanical phenotypes. Our results demonstrate a previously unrecognized class of phenotypes that may be common in cell adhesion and muscle proteins.

Modular proteins that are exposed to mechanical stress play important roles in regulating the elasticity of the extracellular matrix[1–3], mediating cell–cell adhesion[4], in the cytoskeleton[5], and in the passive elasticity of muscle[6–8]. These proteins are typically composed of domains that are placed in tandem. Some of these domains have been found to contain mutations[9–11]. Many of these mutations are thought to change the ligand binding properties (affinity and specificity) of the affected protein modules (for example, mutations in the cell adhesion protein L1; ref. 10), but others remain unexplained[9]. It is likely that many of these mutations change the mechanical stability of the modules. However, it has not been possible to investigate how mutations affect resistance to mechanical unfolding (mechanical stability) until now.

Here we demonstrate the effects of point mutations on the mechanical stability of a protein module. Our experiments made use of recently developed single molecule atomic force microscopy (AFM)[12–16] and protein engineering techniques[12,13,16] to probe the effects of proline mutagenesis on the mechanical stability of the 27th immunoglobulin module of human cardiac titin (I27, following the convention of Labeit and Kolmerer[6]). This protein module serves as an ideal model system for these studies because it has a known structure[17], it has been modeled using steered (or biased) molecular dynamics[18–20] and its mechanical properties have been studied[12–16]. The I27 module consists of 89 amino acids that fold into a characteristic β-sandwich with seven strands[17]. When stretched by an atomic force microscope, a polyprotein composed of I27 modules extends beyond its contour length by sequential unfolding of the individual modules, creating a force-extension curve with a characteristic sawtooth pattern that can be readily recognized and studied[12–16,21].

Steered molecular dynamics simulations of the mechanical unfolding of the I27 module[18,19] have predicted that the major mechanical resistance to unfolding is located in a cluster of backbone hydrogen bonds linking the A′ strand (amino acids 9, 11, 13 and 15) to the G strand (amino acids 83, 85 and 87) (Fig. 1*a*). These predictions are supported by recent AFM experiments[12–14,16] and suggest that any alteration of the atomic interactions in the A′–G overlap region may reduce the mechanical stability of the I27 module. This hypothesis has been tested in this work.

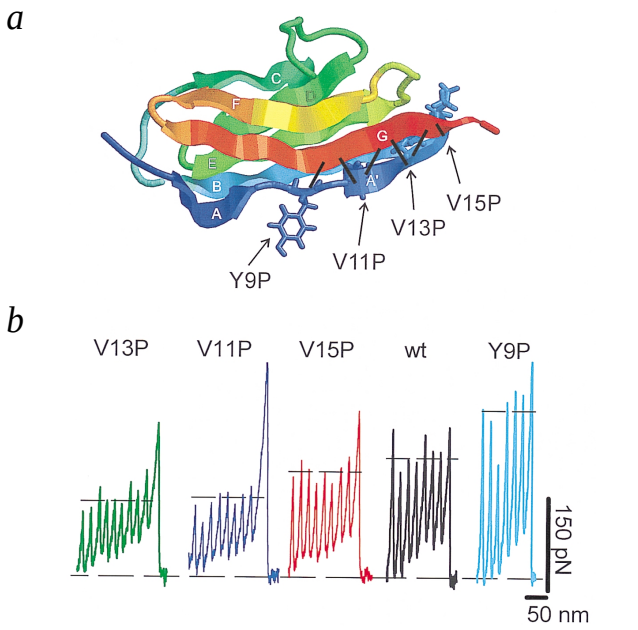

Fig. 1 Point mutations in an immunoglobulin module alter its mechanical stability. ***a***, Cartoon diagram showing the β-sandwich structure of the I27 module and the amino acids that were substituted by Pro residues in this work. Black bars indicate the six backbone hydrogen bonds linking the A′ and G β-strands. ***b***, The force extension relationships for the I27 polyproteins: wild type (black), Y9P (cyan), V11P (blue), V13P (green), and V15P (red) (we use the same color code throughout the paper). The mutations V11P, V13P and V15P decrease the force required to unfold the I27 module (see text). By contrast, the mutation Y9P increases this force. These recordings were obtained at a pulling speed of 0.6 nm ms^{-1}.

Mechanical phenotypes of proline mutants

Because the A′–G overlap of the I27 module is thought to be the major point of mechanical resistance, we have focused our mutation studies on this region of the module (Fig. 1*a*). We used proline mutagenesis to block the formation of specific backbone hydrogen bonds and to disrupt the β-sheet structure within the overlap[22]. We created four point mutants in this region (Y9P, V11P, V13P and V15P) (Fig.1*a*) and used them to construct polyproteins for AFM measurements. A comparison of the force-extension relationships of the wild type polyprotein and the four mutants is shown in Fig. 1*b*. Mutants V11P, V13P and V15P showed reduced unfolding forces (horizontal bars in Fig. 1*b*; V11P, 143 pN, n = 273; V13P, 132 pN, n = 384; V15P, 159 pN, n = 259; average forces given; n is number of observations) compared to the wild type protein (204 pN, n = 266) (Fig. 2*a*). A proline substitution at position 9 resulted in increased unfolding forces (268 pN, n = 340). In addition, the Y9P polyprotein showed a much broader distribution of unfolding forces than the wild type and the other three mutants (Fig. 2*a*). These results demonstrate that point mutations can significantly alter the mechanical properties of an immunoglobulin module.

Unfolding kinetics of Pro mutants

AFM experiments have been used to determine the unfolding distance and the unfolding rate constant for the I27 polyprotein[12,15]. The unfolding force of a module was shown to depend on the pulling speed[12]. The average unfolding force *versus* the pulling speed (0.005–6 nm ms^{-1}) for the wild type and mutant I27 polyproteins is plotted in Fig. 2*b*. The data show that the average unfolding force for the mutant polyproteins V11P, V13P and V15P has a much weaker dependence on the pulling speed than that of

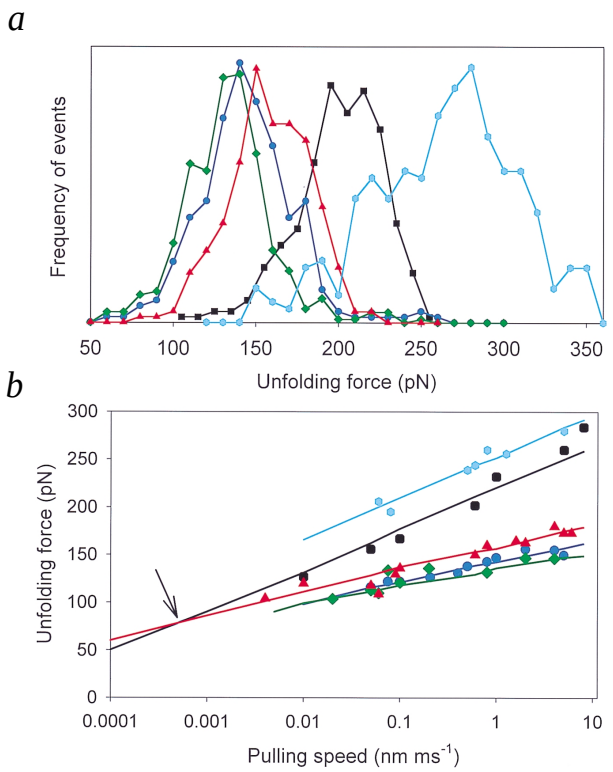

Fig. 2 Magnitude and kinetics of forced unfolding of mutant proteins. ***a***, Unfolding force frequency histograms for the wild type (wt) and the mutant I27 polyproteins. The pulling speed was 0.6–0.8 nm ms^{-1}. The width of the histograms reflects the stochastic nature of the unfolding process. Although some of the scatter may be due to errors in the force measurements (~20 pN), most is due to the probabilistic nature of the unfolding process[12]. ***b***, A plot of the average unfolding force *versus* the pulling speed reveals that Pro substitutions can alter the kinetics of unfolding (changed slope). To quantify these changes we used Monte Carlo simulations to estimate the unfolding rate and the distance to the transition state, as described[12]. The solid lines are fits of the Monte Carlo simulation to the experimental data (see text). The figure also shows that the relative mechanical stability of the mutant proteins depends on the pulling speed. For example, the arrow indicates the crossover pulling speed for the wild type and V15P proteins. Above this speed, wild type proteins are more stable than V15P mutants, below this speed V15P mutants are predicted to be more stable than the wild type protein.

the wild type. By contrast, the unfolding of the Y9P mutant shows a dependence on the pulling speed that is similar to that of the wild type protein.

Unfolding is modeled as a two-state process — that is, only the folded and the unfolded states are populated in the reaction. The unfolding rate constant $\alpha(F)$ is expressed as $\alpha_0 \exp(F\Delta x_u / kT)$, where F is the applied force, α_0 is the unfolding rate constant without the applied force, Δx_u is the unfolding distance, k is the Boltzmann constant and T is the temperature in K. The Monte Carlo approach was used to estimate the α_0 and Δx_u values and to generate a set of simulated sawtooth patterns over the experimental range of pulling speeds[12,15,23]. The average unfolding force obtained from the simulations was then plotted as a function of the pulling speed and compared with the experimental data (Fig. 2*b*, solid lines). Using a previously described procedure[12], the values of α_0 and Δx_u in the Monte Carlo simulation were adjusted until the simulated relationship between unfolding force and pulling speed matched the experimental data of Fig. 2*b*. We found that the average unfolding force and its speed dependence were adequately reproduced using the following values for α_0 and Δx_u: Y9P, $\alpha_0 = 5 \times 10^{-5}$ s^{-1}, $\Delta x_u = 0.25$ nm; V11P, $\alpha_0 = 7 \times 10^{-6}$ s^{-1}, $\Delta x_u = 0.50$ nm; V13P, $\alpha_0 = 8 \times 10^{-7}$ s^{-1}, $\Delta x_u = 0.60$ nm; V15P, $\alpha_0 = 7 \times 10^{-6}$ s^{-1}, $\Delta x_u = 0.45$ nm. The point mutations V11P, V13P and V15P reduce the force required to unfold the I27 protein module. However, the Monte Carlo simulations predict that at lower speeds (<0.001 nm ms^{-1}) these mutants may require higher forces to unfold than the wild type I27. For example, the arrow in Fig. 2*b* indicates the crossover pulling speed for the wild type and V15P proteins. This result clearly demonstrates that the effect of a point mutation on the mechanical stability of a protein module cannot be defined at a single pulling speed.

The unfolding rate constants of the four mutants measured by the Monte Carlo technique are smaller than that of the wild type (3.3×10^{-4} s^{-1}), indicating that the activation energy of unfolding was increased by the proline mutations. The unfolding distance of the Y9P protein is identical to that of the wild type (0.25 nm), while the unfolding distances of the other three mutants are considerably longer. This result indicates that mutation of amino acids 11, 13 or 15 to Pro affects the position of the transition state along the reaction coordinate (distance), shifting it towards the unfolded state of the module.

Refolding kinetics of Pro mutants

By stretching and relaxing the same polyprotein repeatedly, with variable intervals between relaxation and stretching, we can measure the time dependence of refolding after a mechanical unfolding event[3,12]. Such an experiment, in which a single polyprotein was repeatedly unfolded and then allowed to refold after a time interval (Δt) is shown in Fig. 3. A plot of the fraction of refolded modules as a function of Δt, for the wild type and the mutant polyproteins, is shown in Fig. 3*b*. Polyprotein refolding is well described by a single exponential. The mutant polyproteins V11P, V13P and V15P fold at the same rate ($\beta_0 = 2.8$ s^{-1}), which is higher than that of the wild type ($\beta_0 = 1.2$ s^{-1}). We were unable to observe refolding of the Y9P polyprotein because this protein, for unknown reasons, detached from the probe before a refolding series of stretch/relaxation cycles could be completed.

Module refolding has been shown to depend on the force applied to the polypeptide chain[3,12,21]. The sensitivity of the refolding rate to an applied force has been used to estimate the refolding distance, an important component of the mechanical energy landscape of the protein[12].

In a typical refolding experiment, a polyprotein is first stretched nearly its contour length, L, to mechanically unfold its modules. Then the protein is relaxed to allow refolding. In order to apply a force during refolding, we relaxed the protein not to its fully relaxed length but to a length L_0, which determines the magnitude of the resulting force that can be calculated from the worm-like chain (WLC) model[12]. After a 5 s interval we again stretched the protein in order to count the number of modules that had refolded (Fig. 3*c*). As had been reported[12], we found that the number of modules that refolded decreased sharply when force was applied. We found that the refolding distance (Δx_f) determined from this plot using Monte Carlo simulations[12] was 2.3 nm for wild type I27 and that this distance remained unchanged by the introduction of the proline mutations (Fig. 3*d*). However, the scatter in the data is such that we can only specify the folding distance within a 0.6 nm margin of error (solid lines in Fig. 3*d*).

Free energy of mechanical folding/unfolding

The kinetic parameters — unfolding rates and distances (α_0, Δx_u) as well as the refolding rates and distances (β_0, Δx_f) — of the wild type and mutant I27 polyproteins extracted from the experiments

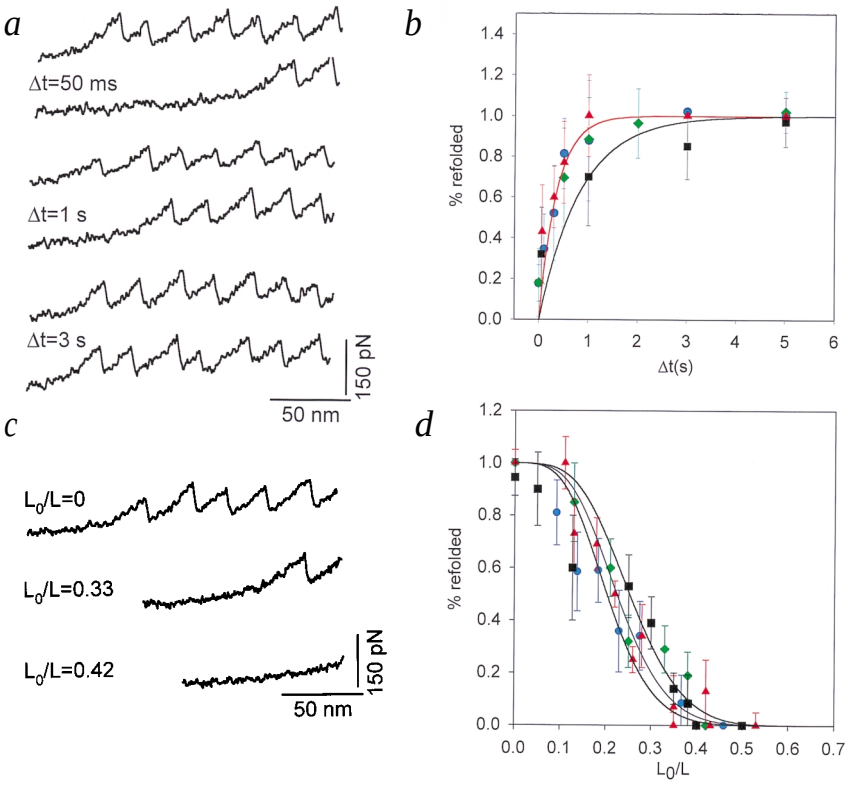

Fig. 3 Refolding kinetics of the I27 polyproteins. ***a***, Unfolding and refolding cycles for a single V11P polyprotein. The protein was first stretched to almost its contour length to count the number of domains that unfolded (N_{total}) and then it was relaxed to its initial length to allow refolding. A second extension after a delay (Δt) measured the number of domains that refolded ($N_{refolded}$). ***b***, Plot of the fraction of refolded domains, $N_{refolded}$ / N_{total} *versus* Δt. The mutant polyproteins all refolded faster than the wild type. The solid lines are fits of the data to the single exponential function $P_f(t) = 1\text{-}e^{-t\beta}$; the refolding rate $\beta = 1.2\ s^{-1}$ for wild type (black line) and $\beta = 2.8\ s^{-1}$ for the mutants (red line). ***c***, The extent of refolding of a polyprotein depends on its residual tension. A polyprotein is first stretched to count the number of domains that unfold (N_{total}) and is then rapidly relaxed to a length L_0 for a fixed period of 5 seconds. L_0 / L (where L is the contour length) determines the residual force applied to the protein during refolding[12]. A second extension measures the number of domains that refolded under the residual tension ($N_{refolded}$). ***d***, Plot of $N_{refolded}$ / N_{total} *versus* L_0 / L. The black solid lines correspond to the Monte Carlo simulations with folding distances $\Delta x_f = 2.0$, 2.3 and 2.6 nm (from left to right).

can be assembled to describe the free energy diagram for the mechanical unfolding/refolding of the I27 polyproteins (Fig. 4), assuming that the reaction proceeds *via* a two-state mechanism.

The changes in activation energy ($\Delta\Delta G_u$) and the changes in the distance to the transition state ($\Delta\Delta x_u$) caused by the proline mutations are shown in Fig. 4. These mutations typically shift the position of the transition state towards the denatured state and increase the activation energy of unfolding while decreasing the activation energy of refolding. It is striking that while the mutations increase the thermodynamic stability of the proteins as well as the height of the activation energy barrier for unfolding, the mutant polyproteins V11P, V13P and V15P unfold at lower forces. It is clear from these data that measuring the thermodynamic stability of a protein may not sufficiently determine its mechanical stability.

Our results show that point mutations in an immunoglobulin module can affect the free energy of mechanical unfolding and the position of the transition state (Fig. 4). Typically, these changes are expressed as $\Delta\Delta G_u$ and $\Delta\Delta x_u$ (Fig. 4) and are summarized in Table 1. There is no simple explanation for the effect of a mutation on the mechanical resistance to unfolding since a mutation can either increase or decrease the unfolding force, depending on the pulling speed (Fig. 2*b*). The data summarized in Table 1 provide an indication of the effect of a mutation on the mechanical stability (ΔF) of the I27 polyprotein at a particular pulling speed. However, it is not obvious in what way the mutation will affect the mechanical stability under a different set of experimental conditions. A unified analytical treatment is needed and will be discussed elsewhere.

Table 1 Mechanical stability of proline mutants

Mutant	$\Delta\Delta G_u$ (kcal mol^{-1})	$\Delta\Delta x_u$ (nm)	ΔF (pN)[1]
Y9P	+1.1	0	+64
V11P	+2.3	+0.25	-61
V13P	+3.6	+0.35	-72
V15P	+2.3	+0.20	-45

[1]At a pulling speed of 0.6 nm ms^{-1}.

Steered molecular dynamics simulations predicted that the force required to unfold the I27 module was determined mainly by the simultaneous rupture of a set of backbone hydrogen bonds in the A′–G overlap[18,19]. Therefore, any disruption of the A′–G overlap is expected to weaken the I27 protein module. This hypothesis is supported by the mutations V11P, V13P and V15P, which decrease the mechanical stability of the I27 module. However, the increased mechanical stability of the Y9P mutant was unexpected. These experiments suggest that proline substitutions not only disrupt hydrogen bonding but also affect or introduce other types of noncovalent interactions that contribute to the mechanical stability of the I27 module. The atomic basis of the changes in the position of the transition state is not known. Developing a detailed theoretical model of all the interactions in the A′–G overlap is, therefore, of great importance for understanding the design of a region that resists mechanical forces in a protein module.

Physiological significance of point mutations

The simplest view of the mechanical properties of titin proposes that its elasticity is solely the result of the thermal fluctuations of the protein that drive it to coil to maximize its entropy[7,8]. If this is true, extension of the protein generates a recoiling force that is simply predicted by the WLC model of polymer elasticity and is solely dependent on its extension within a fixed contour length[7,8]. In other words, instead of a sawtooth pattern, a force extension relationship would simply show a monotonically increasing function given by the WLC relationship. From this point of view, a point mutation is just an inconsequential alteration of the polymer chain.

In contrast to this hypothesis, recent single molecule force spectroscopy experiments have revealed that titin is a complex molecule and that it does not behave as a simple entropic spring[21,24,25]. As first suggested by Erickson[1], the single molecule experiments demonstrated that the tandem immunoglobulin modules of titin unfold under force. These experiments also showed that the titin

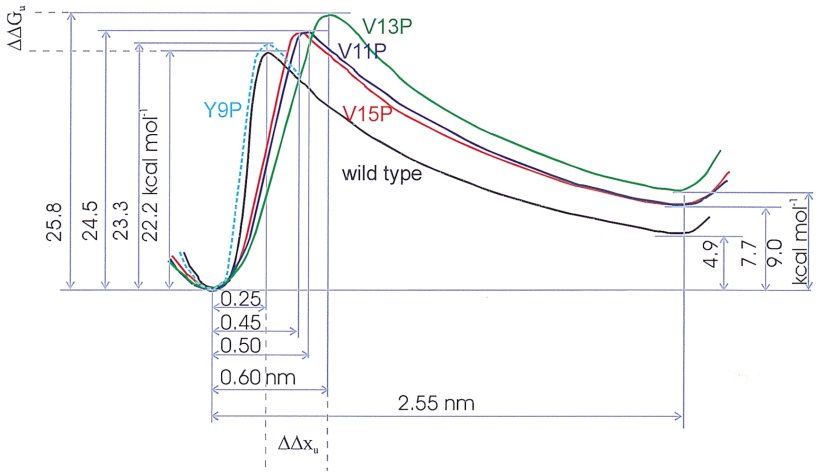

Fig. 4 Free energy diagram for the mechanical unfolding and refolding of the I27 module and its mutants. This schematic was calculated from the single molecule AFM experiments described in the text. The free energies were calculated from the rate constants for unfolding and refolding at zero force (α_0, β_0; see Methods). In this diagram we have assumed that the total distance between the native and the unfolded states remains constant ($\Delta x = \Delta x_u + \Delta x_f = 2.55$ nm) and that all the native states have a common origin. The figure reveals that the positions of the transition state for the V11P, V13P and V15P modules are significantly shifted towards the unfolded state. By contrast, the position of the transition state of the Y9P mutant is the same as that of the wild type. All mutations increase the kinetic stability of the protein as indicated by the increased height of the unfolding energy barrier. From the refolding rate constants we also calculate that Pro mutants increase thermodynamic stability. However, these mutations cause a decrease in mechanical stability.

modules have varying mechanical stability, which determines which modules unfold at a given force and pulling speed[15,21]. These observations may have implications on the biological functions of titins. For example, the elastic I band region of human cardiac titin contains 42 tandem immunoglobulin modules[6]. A folded module has a length of 4.4 nm[17], whereas unfolding of a single immunoglobulin module lengthens a titin molecule abruptly by ~28 nm and immediately relaxes the stretching force[12,21,25]. The unfolding of only two or three titin immunoglobulin modules per molecule is sufficient to account for the relaxation of the stretching force in an intact muscle fiber (ref. 25; A. Minajeva, M. Ivemeyer, J.M.F. & W.A. Linke, unpublished results). The number and timing of unfolding events may thus control the operating contour length of I band titin[24]. Our data predict that point mutations in immunoglobulin modules have the potential for disrupting the finely tuned elasticity of human cardiac titin and may result in yet unrecognized forms of familial cardiomyopathy.

Immunoglobulin modules are also common components of cell adhesion proteins, which play important roles in development, tissue formation and inflammation[9]. The mechanical effects of point mutations in an immunoglobulin module, as demonstrated here, may help understand the molecular mechanisms underlying the physiological effects of mutations that target cell adhesion proteins.

Methods

Engineering wild type and mutant I27 polyproteins. We used recombinant DNA techniques to synthesize and express direct tandem repeats of I27 monomers[12]. Point mutations were introduced by PCR using standard techniques. All engineered polyproteins were expressed in the recombination defective strain BLR (DE3) (Novagene), purified by Ni^{2+} affinity chromatography and kept at 4 °C in PBS (phosphate buffer saline), 5 mM DTT (dithiothreitol), 0.2 mM EDTA buffer.

Atomic force microscopy. Details of the custom-made AFM apparatus had been described previously[3,12–16]. Calibration of the cantilevers (Si_3N_4 twin-tips from Digital Instruments, Inc.) was done in solution and using the equipartition theorem as described[26,27]. The spring constant of the cantilever (~100 mN m^{-1}) is determined with 20% accuracy using the method described in ref. 27.

Monte Carlo simulations. The distribution (Fig. 2*a*) and speed dependency (Fig. 2*b*) of the unfolding forces were fit using Monte Carlo simulation to calculate the unfolding rate constants and the position of the transition state[12,23]. The folding/unfolding of a domain was modeled as a two-state Markovian process. The probability of unfolding was $P_u = N_f \alpha \Delta t$, where N_f is the number of folded modules and Δt is the polling interval, defined as the total time of the simulation divided by the number of Monte Carlo trials. The folding probability was $P_f = N_u \beta \Delta t$, where N_u is the number of unfolded modules. The rate constants for unfolding (α) and refolding (β) are given by $\alpha = \alpha_0 \exp(F\Delta x_u / kT)$ and $\beta = \beta_0 \exp(-F\Delta x_f / kT)$, where F is the applied force and Δx_u and Δx_f are the unfolding and folding distances, respectively. β_0, the folding rate in the absence of an applied force, was obtained from Fig. 3*b*. During the forced unfolding simulations β was set to zero (see reference 12 for details). The force due to the extension of the protein was calculated from the worm like chain model of polymer elasticity with the parameters: contour length, L_c and persistence length, p[12,23]. L_c was calculated from the number of unfolded and folded modules during the Monte Carlo simulation. The persistence length of the polypeptide chain was always set to 0.4 nm.

Acknowledgments

We thank C. Badilla-Fernandez and J. Kerkvliet for their help in polyprotein engineering. This work was supported by National Institute of Health grants to J.M.F.

Correspondence should be addressed to J.M.F. email: fernandez.julio@mayo.edu

Received 9 June, 2000; accepted 10 October, 2000.

1. Erickson, H.P. *Proc. Natl. Acad. Sci. USA* **91**, 10114–10118 (1994).
2. Ohashi, T., Kiehart, D.P. & Erickson, H.P. *Proc. Natl. Acad. Sci. USA* **96**, 2153–2158 (1999).
3. Oberhauser, A.F., Marszalek, P.E., Erickson, H.P. & Fernandez, J.M. *Nature* **393**, 181–185 (1998).
4. Casasnovas, J.M., Stehle, T., Liu, J.H., Wang, J.H. & Springer, T.A. *Proc. Natl. Acad. Sci. USA* **95**, 4134–4139 (1998).
5. Rief, M., Pascual, J., Saraste, M. & Gaub, H.E. *J. Mol. Biol.* **286**, 553–541 (1999).
6. Labeit, S. & Kolmerer, B. *Science* **270**, 293–296 (1995).
7. Linke, W.A. *et al. J. Cell Biol.* **146,** 631–644 (1999).
8. Trombitas, K.M. *et al. J. Cell Biol.* **140**, 853–859 (1998).
9. Chothia, C. & Jones E.Y. *Annu. Rev. Biochem.* **66**, 823–862 (1997).
10. Bateman, A. *et al. EMBO J.* **15**, 6050–6059 (1996).
11. Kenwrick, J.J. In *Ig superfamily molecules in the nervous system.* (ed., Sonderegger, P.) 287–303 (Harwood, Amsterdam; 1998).
12. Carrion-Vazquez, M. *et al. Proc. Natl. Acad. Sci. USA* **96**, 3694–3699 (1999).
13. Carrion-Vazquez, M., Marszalek, P.E., Oberhauser, A.F. & Fernandez, J.M. *Proc. Natl. Acad. Sci. USA* **96**, 11288–11292 (1999).
14. Oberhauser, A.F., Marszalek, P.E., Carrion-Vazquez, M. & Fernandez, J.M. *Nature Struct. Biol.* **6**, 1025–1028 (1999).
15. Li, H.B., Oberhauser, A.F., Fowler, S.B., Clarke, J. & Fernandez, J.M. *Proc. Natl. Acad. Sci. USA* 97, 6527–6531 (2000).
16. Marszalek P.E. *et al. Nature* **402**, 100–103 (1999).
17. Improta, S., Politou, A.S. & Pastore, A. *Structure* **4**, 323–337 (1996).
18. Lu, H., Isralewitz, B., Krammer, A., Vogel, V. & Schulten, K. *Biophys. J.* **75**, 662–671 (1998).
19. Lu, H. & Schulten, K. *Biophys. J.* **79**, 51–65 (2000).
20. Paci, E. & Karplus, M. *Proc. Natl. Acad. Sci. USA* **97**, 6521–6526 (2000).
21. Rief, M., Gautel, M., Oesterhelt, F., Fernandez, J.M. & Gaub, H.E. *Science* **276**, 1109–1112 (1997)
22. Wood, S.J., Wetzel, R., Martin, J.D. & Hurle, M.R. *Biochemistry* **34**, 724–730 (1995).
23. Rief, M., Fernandez, J.M. & Gaub H.E. *Phys. Rev. Lett.*, **81**, 4764–4767 (1998)
24. Kellermayer, M., Smith, S., Granzier, H. & Bustamante, C. *Science* **276**, 1112–1116 (1997).
25. Tskhovrebova, L., Trinick, J., Sleep, J.A. & Simmons, R.M. *Nature* **387**, 308–312 (1997).
26. Hutter, J.L. & Bechhoffer, J. *Rev. Sci. Instrum.* **64,** 1868–1873 (1993).
27. Florin, E.L. *et al. Biosens. Bioelectr.* **10**, 895–901 (1995).